Ab initio study of fully relaxed divacancies in GaAs

S. Pöykkö, M. J. Puska, and R. M. Nieminen

Laboratory of Physics, Helsinki University of Technology, FIN-02150 Espoo, Finland

(Received 7 September 1995)

We report calculations of the electronic and atomic structures of neutral and charged divacancies in GaAs using the first-principles Car-Parrinello method. It is found that the divacancy relaxes inwards in all charge states $(2-,1-,0,1+)$ studied. The defect-induced electron levels lie in the lower half of the fundamental band gap. The doubly negative divacancy is the most stable one for nearly all values of the electron chemical potential within the band gap. The deep-level electron density is localized at the Ga-vacancy end of the divacancy and the ionic relaxation is stronger there than at the As-vacancy end. We have also calculated the thermodynamic concentrations for several different native defects in GaAs, and the implications for self-diffusion are discussed.

I. INTRODUCTION

To a great extent the electrical and optical properties of semiconductors are governed by defects, which also exhibit interesting physics of their own. During the recent years point defects in III-V compound semiconductors have been intensively studied both theoretically and experimentally. Among the native defects the main theoretical interest has been oriented towards monovacancies, antisites, and interstitials,[1–4] but also vacancy complexes such as divacancies have been studied.[5–7,3]

Electronic structure calculations indicate that for a Fermi-level position around the midgap the As vacancy is in the singly positive charge state, whereas the Ga vacancy is in the triply negative charge state.[1,3,4] Therefore vacancies in different sublattices feel a mutual Coulomb attraction and the possibility for vacancy pairing arises. The combination of the two vacancies in the above-mentioned charge states leads to the doubly negative divacancy. Indeed, the doubly negative charge state is according to our detailed electronic-structure calculations (see below) the most stable one for the divacancy.

A few experimental results have been used to identify divacancies in GaAs. These works include localized vibrational mode (LVM) spectroscopy (oxygen-related divacancies) (Ref. 8) and positron lifetime measurements.[9] The fact that vacancies created by electron irradiation are associated with the corresponding interstitials (Ga_i, As_i) hampers the divacancy formation: the attraction between the As and Ga vacancies has to compete with the vacancy-interstitial recombination. For example, the pair V_{Ga}-Ga_i is unstable even at the lowest temperatures.[10]

Theoretical studies of divacancies in GaAs (Refs. 5–7) have usually been performed for the ideal divacancy, i.e., by neglecting the ionic relaxation around the defect. For example, Xu[7] has calculated with the semiempirical tight-binding method properties of ideal divacancies in III-V compounds. Very recently, Northrup and Zhang have done a calculation for the divacancy in GaAs with lattice relaxations taken into account,[3] but only for the neutral charge state. Monovacancy studies[2] clearly indicate that lattice relaxation is important and cannot be ruled out even in the case of the

simplest point defects. The divacancy has a much larger open volume and therefore it is expected that lattice relaxation is even more important than for a monovacancy. For example, we find that the lattice relaxation lowers the total energy of the divacancy by 0.5–1.0 eV.

Our aim in this work is to study the electronic and ionic structure of the divacancy in GaAs. Especially, we want to check if the divacancy becomes an important defect in GaAs for certain experimental conditions defined by the position of the Fermi level (doping) and the stoichiometry (growing conditions). For these purposes we perform *ab initio* electronic-structure calculations for the divacancy at different charge states. We also need to calculate the properties of the other native point defects which are known to have small formation energies.[1,3,4] This information is necessary in order to estimate the thermal equilibrium concentrations of divacancies and other defects in a consistent way.

The paper is organized in the following way. In Sec. II we discuss the basic theoretical and computational methods used in calculations. In Sec. III we give a detailed analysis of our results and, finally, the conclusions are given in Sec. IV.

II. THEORY

A. Basic computational methods

Our calculations are made using the Car-Parrinello (CP) method.[11] It is a full *ab initio* method with respect to both electronic and ionic degrees of freedom which are optimized simultaneously by the use of the density functional theory[12] and molecular dynamics. For the valence-electron-ion-core interaction we use the norm-conserving, Bachelet-Hamann-Schlüter-type pseudopotentials.[13] Pseudopotentials are fully separable[14] and the d component is used as a local one for both Ga and As. The valence-electron wave functions are expanded in a plane-wave (PW) basis set and terms corresponding to kinetic energies up to 17 Ry are included, so that for each electron state we have approximately 11 000 PW's. For the Brillouin-zone sampling only the Γ point is used, although some test calculations have been made with larger **k**-point sets. The exchange-correlation energy E_{xc} is calculated within the local density approximation (LDA).[15] In our

calculations a supercell with 64 atomic sites is used. The divacancy is created by leaving two nearest-neighbor sites empty.

We have performed the calculations in two stages. First, static calculations have been made, i.e., ions are kept in their ideal-lattice positions and electrons are relaxed to the corresponding Born-Oppenheimer (BO) surface. After relaxing the electrons to the BO surface the ions are left free to move. Special care is taken in order to keep the electrons close to the BO surface so that the errors in the Hellmann-Feynman forces are small enough to ensure a rapid convergence. We do this by monitoring the fictitious kinetic energy of the electrons: If it is larger than a given cutoff value, the ionic movement is stopped for a while and the electrons are relaxed back to the BO surface. Thereafter the ionic motion is continued in the normal CP fashion. In the beginning of each ionic relaxation process the forces acting on ions are quite large and small errors due to the lack of adiabaticity are not important. When the ions are close to their final positions the Hellmann-Feynman forces are small and errors of the same magnitude may lead to harmful oscillations of the ions around their equilibrium sites. We have implemented an automatic control of the adiabaticity to our code using a relatively small cutoff value for the fictitious kinetic energy of the electrons so that in average after a couple (three to five) of CP steps the electronic structure is corrected by doing a couple (one to three) of purely electronic steps. When these purely electronic steps are taken the forces acting on the ions are not computed, which reduces the time consumption of the calculation. We have found that this small modification to the CP method is very efficient: the number of time steps needed to find the equilibrium configuration is reduced significantly in comparison with the traditional CP method. As a matter of fact, the number of time steps needed for the relaxation of both the ions and electrons is comparable to the number of steps needed to relax the electronic system alone. The efficiency is due to the fact that there is an energy transfer between the electronic and the ionic degrees of freedom and by stopping the ionic motion occasionally and cooling the electronic system we actually cool the ionic system as well.

In Fig. 1 we demonstrate the efficiency of the new adiabatic Car-Parrinello relaxation. The figure shows the evolution of the total energy of the doubly negative divacancy during the ionic relaxation. The iterations start from an ideal divacancy with fully converged electronic structure. In the beginning of the relaxation we use the traditional Car-Parrinello method. The procedure does not lead to a rapid convergence because the ions begin to oscillate around their equilibrium positions and also the total energy oscillates. In order to accelerate the convergence we switch to the procedure where the steepest-descent minimization is employed if the velocity $\mathbf{v}_i$ of an ion and the force $\mathbf{F}_i$ acting on it obey $\mathbf{F}_i \cdot \mathbf{v}_i < 0$. Furthermore, if $\mathbf{F}_i \cdot \mathbf{v}_i > 0$ the traditional Car-Parrinello method is used. As seen in the figure, this combined Car-Parrinello steepest-descent method does not lead to a fast convergence. Finally, we switch to the above described adiabatic Car-Parrinello relaxation leading rapidly and without oscillations to the ground state of the system.

The electronic time step used in our calculations is 1.2×10^{-16}s, the fictitious electron mass is 400 a.u., and the
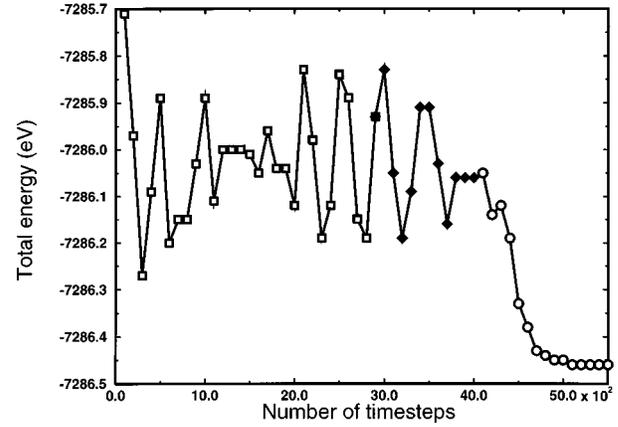
FIG. 1. Evolution of the total energy of the doubly negative divacancy in GaAs during the ionic relaxation. The squares, diamonds, and circles denote the domains of the traditional Car-Parrinello method, the combination of the Car-Parrinello and the steepest-descent methods, and the new adiabatic Car-Parrinello method, respectively.

ion masses are between 5 and 8 amu. The equilibrium lattice constant we obtain is 5.56 Å, i.e., about 2% less than the experimental one, in good agreement with other similar LDA calculations.[16]

B. Energy levels and defect formation energies in supercell calculations

We will now consider the determination of the thermodynamic concentrations for the native defects in GaAs. First, it is necessary to identify the defects with low formation energies for every position of the Fermi level and every possible stoichiometry. We adopt here the formalism by Zhang and Northrup[1] in which the formation energy $\Omega_D(Q)$ of a defect in the charge state Q is considered. In this formalism,

$$\Omega_D(Q) = E_D(Q) + Q(E_V + \mu_e) - n_{Ga}\mu_{Ga} - n_{As}\mu_{As}$$

$$= E_D(Q) - \frac{1}{2}(n_{Ga} + n_{As})\mu_{GaAs(bulk)}$$

$$- \frac{1}{2}(n_{Ga} - n_{As})(\mu_{Ga(bulk)} - \mu_{As(bulk)})$$

$$+ Q(E_V + \mu_e) - \frac{1}{2}(n_{Ga} - n_{As})\Delta\mu, \qquad (2.1)$$

where $E_D(Q)$ is the total energy of the defect supercell in question. n_{Ga} and n_{As} are the numbers of Ga and As atoms in the supercell, respectively. μ_e is the electron chemical potential measured relative to the valence-band maximum E_V. $\mu_{Ga(bulk)}$ and $\mu_{As(bulk)}$ are the chemical potentials of the Ga and As atoms in the bulk Ga and As lattices, respectively. $\mu_{GaAs(bulk)}$ is the chemical potential of the GaAs pair in the bulk GaAs compound. Actually it is possible to know only

$$\mu_{GaAs(bulk)} = \mu_{Ga} + \mu_{As}, \qquad (2.2)$$

not the chemical potentials μ_{Ga} and μ_{As} of the single atom separately. This fact is circumvented in Eq. (2.1) by introducing the chemical potential difference,

$$\Delta\mu = (\mu_{Ga} - \mu_{As}) - (\mu_{Ga(bulk)} - \mu_{As(bulk)}). \quad (2.3)$$

The allowed range of $\Delta\mu$ is determined from the calculated heat of formation for GaAs ΔH defined as

$$\Delta H = \mu_{Ga(bulk)} + \mu_{As(bulk)} - \mu_{GaAs(bulk)}. \quad (2.4)$$

The chemical potential difference $\Delta\mu$ determines the deviation from the ideal stoichiometry; it can vary from $-\Delta H$ (As-rich) to ΔH (Ga-rich).

According to Eq. (2.1) the formation energy of a defect at a (non-neutral) charge state Q depends on the position of the valence-band maximum (VBM) E_V in the defect supercell. In a supercell calculation, due to the finite size effects, the position of the VBM differs in the defect supercell from the position in the perfect crystal. Therefore it is necessary to estimate the proper lineup of the energy levels in order to get the position of the VBM in the defect supercell. Following Garcia and Northrup,[17] we use as the VBM its value from the bulk supercell calculation corrected by the difference between the average potential in a bulklike environment of the defect supercell and the average potential in the ideal bulk supercell, i.e.,

$$E_V = E_{V(bulk)} + V_{average(bulklike)} - V_{average(bulk)}. \quad (2.5)$$

In principle, the last two terms in Eq. (2.5) would cancel each other in the case of a very large supercell. It is, however, impossible to use such a large supercell in the present calculations. In practice, the potential is stored in a three-dimensional (3D) point grid and when calculating the average potentials for Eq. (2.5) one has to choose such points that the averages are calculated over (at least) one conventional (or primitive) unit cell. Finally, we define

$$E'_D(Q) = E_D(Q) - \frac{1}{2}(n_{Ga} + n_{As})\mu_{GaAs(bulk)}$$
$$- \frac{1}{2}(n_{Ga} - n_{As})(\mu_{Ga(bulk)} - \mu_{As(bulk)}) + QE_V$$
$$(2.6)$$

and write Eq. (2.1) in the short form,

$$\Omega_D(Q, \mu_e, \Delta\mu) = E'_D(Q) + Q\mu_e - \frac{1}{2}(n_{Ga} - n_{As})\Delta\mu. \quad (2.7)$$

Using this equation it is easy to calculate the defect formation energies for different material conditions.

The ionization level $([Q+1]/Q)$ of a given defect is defined for a constant $\Delta\mu$ as the position of the Fermi level μ_e at which the charge state of the defect changes from $Q+1$ to Q. This position follows from the fact that for a given μ_e the charge state is determined by minimizing the formation energy. Thus, using Eq. (2.7) one has to solve

$$E'_D(Q) + Q\mu_e = E'_D(Q+1) + (Q+1)\mu_e \quad (2.8)$$

for the Fermi level μ_e.

The thermodynamic concentrations of the different types of defects are calculated from the defect formation energies by using the charge neutrality condition.[1] We neglect the effects due to the formation entropy. The entropy differences

can reach the value of $\sim 3k_B$, which corresponds to ~ 0.20 eV at the temperature of 850 K,[18] and are thus not expected to change the relative defect abundancies qualitatively.

The charge neutrality condition determines the position of the Fermi level. For example, in the case of an effective n-type doping concentration of N_d the charge neutrality condition reads as

$$\sum_{\text{defects}} -Qz_D N_s e^{-\Omega_D(Q, \mu_e, \Delta\mu)/k_B T} + n_e - n_h = N_d, \quad (2.9)$$

where N_s is the number of the sublattice sites per unit volume, and z_D is the number of different possible configurations for a defect per sublattice site. The concentrations of electrons (n_e) and holes (n_h) at a given temperature are calculated from the effective conduction-band and valence-band densities.[19] The determination of the Fermi level μ_e for a given stoichiometry $\Delta\mu$ and doping N_d requires the self-consistent solution of Eqs. (2.7) and (2.9). The charge state Q of the defect is determined in this process by comparing the Fermi level with the ionization levels. Finally, the concentration of a given defect is given by

$$C_D = z_D N_s \exp[-\Omega_D(Q, \mu_e, \Delta\mu)/k_B T]. \quad (2.10)$$

III. RESULTS AND DISCUSSION

A. Electronic structure

First we give a qualitative model for describing the electronic structure of the divacancy in GaAs.[7] The model is based on the hybridization of the six dangling-bond orbitals corresponding to the nearest-neighbor atoms of the divacancy. For the ideal divacancy the point-symmetry group is C_{3V} and therefore the resulting defect states are a_1 singlets and e doublets. Let us assume that the dangling-bond orbitals first hybridize at the two ends of the divacancy (V_{Ga}, V_{As}), separately. As a result, nondegenerate a_1 and doubly degenerate e states corresponding, respectively, to the a_1 and the t_2 states of the isolated vacancy are formed at the Ga and As vacancies. In accordance with the corresponding isolated-vacancy states the e state for the Ga-vacancy end lies in the lower half of the band gap, whereas the a_1 is located in the valence band. Similarly, for the As-vacancy end the e state lies in the upper half of the band gap and the a_1 state lies near the VBM. Next, the a_1 states belonging to the opposite ends of the divacancy hybridize and form bonding and antibonding nondegenerate σ-like a_1 states. The hybridization of the e states belonging to the opposite ends of the divacancy leads to doubly degenerate π-like e states. The schematic view of this model is shown in the inset of Fig. 2. This scheme will be further refined due to the Jahn-Teller–type lifting of the degeneracy of the e states in the case of their partial filling.

In Fig. 2 the actual positions of the occupied single-particle energy levels from our calculations are given for different charge states. The number of electrons on each level is also shown. The electronic structures obtained follow the qualitative model explained above. The doubly negative divacancy has a fully occupied bonding (π-like) e state in the lower half of the band gap and a fully occupied antibonding (σ-like) a_1 state just above the VBM. Due to the full
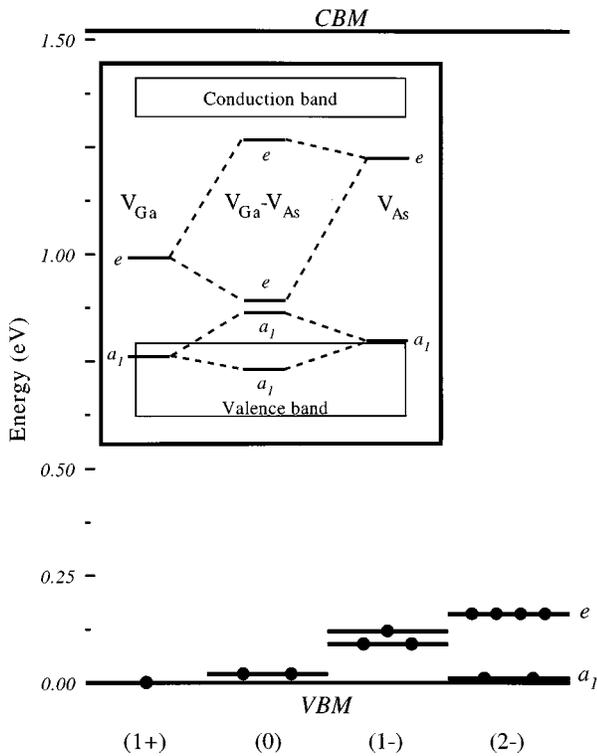
FIG. 2. Single-particle energy levels for the deep electron states at the divacancy in GaAs. The figure shows the positions and occupancies of the energy levels according to our calculations. The top of the valence band defines the energy zero. The inset is a qualitative model based on the hybridization of the a_1 and e states corresponding to the Ga and As vacancies in the C_{3V} point symmetry.

occupancy of the e state the ionic relaxation conserves the C_{3V} symmetry of the ideal divacancy and the degeneracy of the e state. The electron density on the deep levels is mainly localized at the Ga-vacancy end as shown in Fig. 3. In the case of the neutral divacancy this leads to a dipole moment of ~ 3 a.u. Because the bond distance in GaAs is 4.63 a.u., the magnitude of the dipole moment indicates a charge transfer of the order of one electron from the surroundings of the As vacancy to that of the Ga vacancy. This dipole moment should lead to optically activated ionic vibrations localized around the divacancy. The positions of the deep levels in the band gap sink when the divacancy becomes more positive. At the same time the Jahn-Teller effect lifts the degeneracy of the e state. As a result the defect-induced levels for the neutral and singly positive divacancies are very close to the VBM. Therefore the existence of any higher positive charge states for the GaAs divacancy is very unlikely.

According to our calculations a divacancy has only neutral and negative charge states. The ionization levels for the defects are calculated using Eq. (2.8). The divacancy has two ionization levels just above the VBM. The charge state changes from 0 to $1-$ when the Fermi level is 0.12 eV above the VBM and from $1-$ to $2-$ at 0.19 eV above the VBM.

B. Lattice relaxations

The ionic relaxation patterns for the GaAs divacancy in different charge states can be inferred from Table I, which
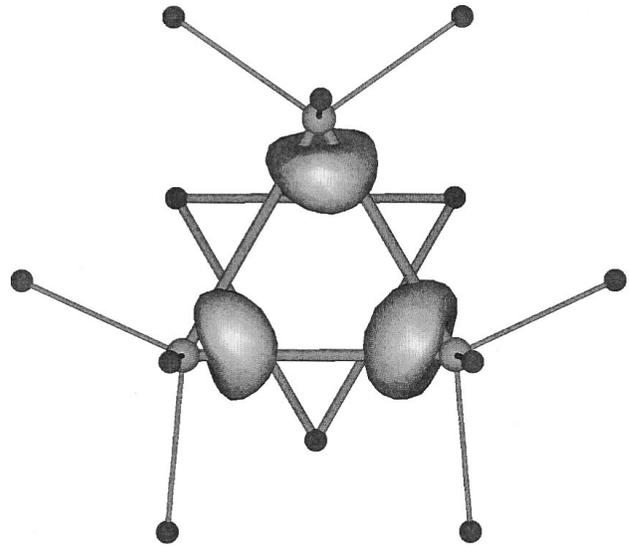
FIG. 3. Deep-level electron density for the doubly negative divacancy in GaAs. The view is along the axis of the divacancy. The large and small spheres denote the As and Ga ions, respectively. The surface corresponding to the density of 1.8 electrons per bulk GaAs unit cell is shown.

gives the distances between the Ga atoms and between the As atoms neighboring the divacancy. On the average the distances become shorter and thus the open volume at the divacancy smaller when the number of bound electrons increases. In the case of the doubly negative divacancy the relaxation pattern conserves the C_{3V} symmetry. The interatomic distances between the As atoms (at the Ga-vacancy end) are slightly shorter than those between the Ga atoms (at the As-vacancy end). This pattern reflects the localization of the deep-level electron density at the Ga-vacancy end (see Fig. 3). It is also in accordance with the results for the monovacancies given for comparison in Table II. Namely, the ionic relaxation is stronger for the isolated triply negative Ga vacancy with six localized electrons than for the isolated singly positive As vacancy with no localized electrons.

For other than the doubly negative charge state of the divacancy the symmetry is lower, σ_{1V}. This means that, as shown in Fig. 4, there is only one mirror plane and it is vertical with respect to the axis of the divacancy. According to Table I the relaxation pattern at the Ga-vacancy end is of the usual Jahn-Teller type, i.e., one of the distances between the neighboring As atoms is shorter than the two others which are equal. At the As-vacancy end it is interesting to note that one of the distances between the Ga atoms is longer than the two equal ones. This kind of relaxation pattern has been recently found in the calculations for the singly negative divacancy in Si.[20] The pattern is called the resonating bond model, because it corresponds to two equal bonds within two pairs of atoms. The model can explain experimental results obtained by the electron paramagnetic resonance method.[20] In the present case the importance of the resonating bond character at the As-vacancy end is small and its possible verification might be quite difficult because the deep-level electron density is mainly localized at the Ga-vacancy end.

The relaxation amplitudes of the nearest-neighbor atoms for some important point defects are given in Table II. The

TABLE I. Nearest-neighbor-ion relaxations for the GaAs divacancy in different charge states. An inward relaxation is found in all charge states studied. The ideal distance between nearest neighbors is 3.93 Å. The numbering of the atoms corresponds to the geometries shown in Fig. 4.

| Defect | As-vacancy end | | Ga-vacancy end | |
symmetry	Pair	Distance (Å)	Pair	Distance (Å)
$(V_{Ga}\text{-}V_{As})^{1+}$	$Ga_1\text{-}Ga_2$	3.54	$As_1\text{-}As_2$	3.57
σ_{1V}	$Ga_2\text{-}Ga_3$	3.76	$As_2\text{-}As_3$	3.57
	$Ga_3\text{-}Ga_1$	3.57	$As_3\text{-}As_1$	3.54
$(V_{Ga}\text{-}V_{As})^{0}$	$Ga_1\text{-}Ga_2$	3.54	$As_1\text{-}As_2$	3.57
σ_{1V}	$Ga_2\text{-}Ga_3$	3.76	$As_2\text{-}As_3$	3.57
	$Ga_3\text{-}Ga_1$	3.54	$As_3\text{-}As_1$	3.53
$(V_{Ga}\text{-}V_{As})^{1-}$	$Ga_1\text{-}Ga_2$	3.59	$As_1\text{-}As_2$	3.56
σ_{1V}	$Ga_2\text{-}Ga_3$	3.67	$As_2\text{-}As_3$	3.56
	$Ga_3\text{-}Ga_1$	3.59	$As_3\text{-}As_1$	3.54
$(V_{Ga}-V_{As})^{2-}$	$Ga_1\text{-}Ga_2$	3.62	$As_1\text{-}As_2$	3.54
C_{3v}	$Ga_2\text{-}Ga_3$	3.62	$As_2\text{-}As_3$	3.54
	$Ga_3\text{-}Ga_1$	3.62	$As_3\text{-}As_1$	3.54

exact definition of the relaxation components can be found in the paper by Laasonen, Nieminen, and Puska.[2] Briefly, the negative breathing mode amplitudes indicate that for the monovacancies and the Ga_{As} antisite the nearest-neighbor atoms relax inwards, towards the center of the defect. The positive breathing mode amplitude in the case of the As_{Ga} antisite means that the nearest neighbors relax outwards from the center of the defect. In the case of the neutral and singly negative As vacancy the Jahn-Teller effect lowers the symmetry so that a pairing component appears. For the singly negative As vacancy this pairing component causes the four atoms neighboring the vacancy to move in pairs closer to each other; for the neutral As vacancy the effect is not so strong. The relaxation patterns given in Table II are in good qualitative agreement with similar recent pseudopotential calculations[2,16,21] and also with recent tight-binding calculations.[4]

C. Formation energies and thermodynamic concentrations

In order to study the importance of the divacancy in GaAs as a thermal equilibrium defect we have determined its for-

TABLE II. Nearest-neighbor-ion relaxations for simple native defects in GaAs. The relaxation modes are defined in the paper by Laasonen, Nieminen, and Puska (Ref. 2). The relaxations are given in percents of the ideal lattice bond distance. The pairing mode 2 is zero for all the defects listed.

Defect	Breathing mode	Pairing mode 1
V_{Ga}^{3-}	-9.5	0.0
V_{As}^{1+}	-1.6	0.0
V_{As}^{0}	-3.7	1.9
V_{As}^{1-}	-17.3	-18.2
Ga_{As}^{2-}	-4.7	0.0
As_{Ga}^{2+}	1.9	0.0
As_{Ga}^{0}	6.4	0.0

mation energy and concentration for various material conditions. The calculations for the other native point defects are needed for the determination of the divacancy concentration.

The formation energies of the simple native defects and of the divacancies in different charge states can be determined according to Eq. (2.7) and the calculated values of $E'_D(Q)$ given in Table III. For the range of the electron chemical potential μ_e we use the experimental width of the band gap. The range of the parameter $\Delta\mu$ is determined by the heat of formation ΔH of the GaAs compound from pure Ga and As solids. According to our calculations, ΔH for GaAs is 1.11 eV. This is slightly larger than the experimental value of 0.74 eV (Ref. 22), but close to the value (1.05 eV) obtained by Northrup and Zhang.[1]
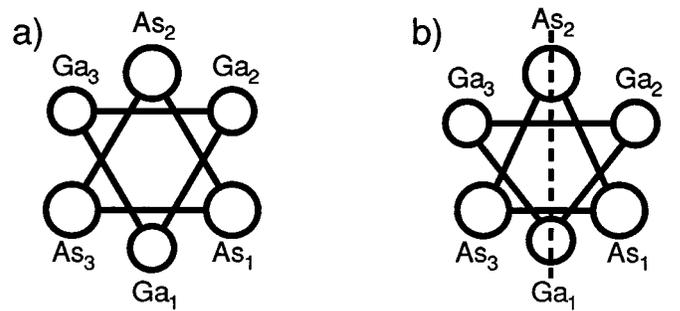
FIG. 4. Relaxation modes for the divacancy in GaAs. The view is along the axis of the divacancy. (a) The symmetry-conserving relaxation mode. The As ions neighboring the Ga-vacancy end relax more strongly inwards than the Ga ions neighboring the As-vacancy end. (b) The symmetry-lowering relaxation mode. The relaxation at the Ga-vacancy end is of the Jahn-Teller type, i.e., the $As_1\text{-}As_2$ and $As_2\text{-}As_3$ distances are equal and longer than the $As_1\text{-}As_3$ distance. The relaxation at the As-vacancy end is of the resonant-bond type, i.e., the $Ga_1\text{-}Ga_2$ and $Ga_1\text{-}Ga_3$ distances are equal and shorter than the $Ga_2\text{-}Ga_3$ distance. The mirror plane is indicated as a dashed line.

TABLE III. Formation energies for native defects in GaAs. The values of the parameters needed in Eq. (2.7) are given.

Defect	E'_D (eV)	$-\frac{1}{2}(n_{Ga}-n_{As})\Delta\mu$	$Q_D\mu_e$
$(V_{Ga}\text{-}V_{As})^{1+}$	3.55	0	μ_e
$(V_{Ga}\text{-}V_{As})^{0}$	3.54	0	0
$(V_{Ga}\text{-}V_{As})^{1-}$	3.66	0	$-\mu_e$
$(V_{Ga}\text{-}V_{As})^{2-}$	3.85	0	$-2\mu_e$
V_{Ga}^{3-}	4.25	$(1/2)\Delta\mu$	$-3\mu_e$
V_{As}^{1+}	1.04	$(-1/2)\Delta\mu$	μ_e
V_{As}^{0}	2.33	$(-1/2)\Delta\mu$	0
V_{As}^{1-}	2.76	$(-1/2)\Delta\mu$	$-\mu_e$
Ga_{As}^{2-}	2.56	$-\Delta\mu$	$-2\mu_e$
As_{Ga}^{2+}	2.33	$\Delta\mu$	$2\mu_e$
As_{Ga}^{0}	2.29	$\Delta\mu$	0

FIG. 5. Equilibrium defect concentrations in GaAs. The concentrations are shown for the most abundant native defects in an n-type material (donor concentration $N_d=10^{18}$cm^{-3}) at the temperature of 853 K.

The total energies used in calculating ΔH are also needed for the determination of the energies $E'_D(Q)$[Eq. (2.6)]. The present defect formation energies given in Table III are, with the exception of As_{Ga}^{2+}, somewhat lower than the values reported by Northrup and Zhang.[23] The calculations by Northrup and Zhang differ from the present one in that they have used a smaller supercell of 32 atoms, a lower cutoff energy of 8 Ry but two special **k** points. The absolute values of the formation energies are, however, less important; what really matters in estimating the thermodynamic concentrations are the formation energy differences. The formation energy differences calculated from the results by Northrup and Zhang are quite close to ours in the case of simple point defects.

From the formation energies given in Table III one can directly calculate that the binding energy of the doubly negative divacancy relative to the triply negative Ga vacancy and singly positive As vacancy is 1.44 eV. Thus, if the migrating Ga and As vacancies come close to each other, they are strongly bound as a divacancy. The attractive Coulomb interaction between the monovacancies of different charges also favors the divacancy formation. The binding energy is, however, much larger than the electrostatic Coulomb interaction between two point charges placed in neighboring lattice sites, indicating that the binding mechanism is not due to a Coulomb force, but due to a covalent one. The strong binding may increase the divacancy concentration in nonequilibrium conditions, such as in electron irradiation.

The formation energies together with the charge neutrality condition can be used to estimate the equilibrium concentration of defects under various conditions. We find that the formation of divacancies is most favorable in n-type materials. For example, in Fig. 5 we show the equilibrium defect concentrations for n-type GaAs with the donor concentration of $N_d=10^{18}$cm^{-3} at the temperature of 853 K, which is a typical growing temperature for GaAs. It is seen that the triply negative Ga vacancy dominates at the As-rich conditions whereas the doubly negative Ga$_{As}$ antisite is the most abundant defect for Ga-rich samples. The maximum thermodynamic concentration of the divacancy is, however, several orders of magnitude smaller than the concentrations of the simpler point defects.
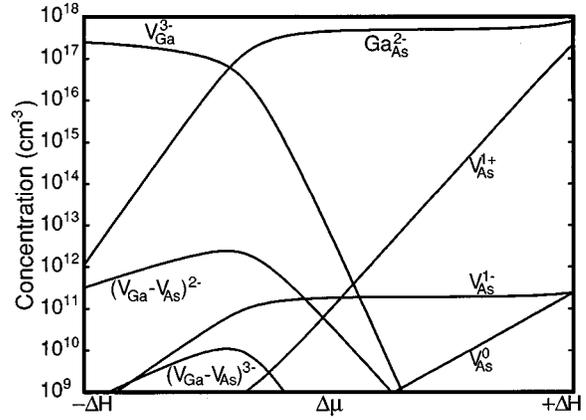
The atomistic picture of self-diffusion in compound semiconductors poses interesting questions. The usual vacancy mechanism with nearest-neighbor jumps seems to be ruled out, as it would lead to a string of antisites following the atomic motion.[24] Divacancy motion would avoid this. However, our results predict such low equilibrium divacancy concentrations that they cannot have a large effect on self-diffusion.

IV. CONCLUSIONS

We have performed first-principles calculations for the electronic and ionic structures of the divacancy in GaAs. The dominant charge state of the divacancy is the doubly negative one and the electronic structure is characterized by deep electron states close to the top of the valence band and localized at the Ga-vacancy end of the divacancy. The distribution of the deep electrons is also reflected in the ionic relaxation, which for the nearest-neighbor ions is inwards to the defect center, and is stronger at the Ga-vacancy end than at the As-vacancy end. Under typical experimental conditions the formation energy for the divacancy in bulk GaAs is higher than that for the simpler native defects. Therefore the equilibrium divacancy concentrations are relatively low. On the other hand, Ga and As monovacancies present in the crystal can form bound pairs with the binding energy of 1.44 eV.

[1] S. B. Zhang and J.E. Northrup, Phys. Rev. Lett. **67**, 2339 (1991).

[2] K. Laasonen, R. M. Nieminen, and M. J. Puska, Phys. Rev. B **45**, 4122 (1992).

[3] J. E. Northrup and S. B. Zhang, Phys. Rev. B **50**, 4962 (1994).

[4] H. Seong and L. J. Lewis, Phys. Rev. B **52**, 5675 (1995).

[5] T. L. Reinecke, Physica B+C **117B & 118B**, 194 (1983).

[6] G. A. Baraff and M. Schlüter, Phys. Rev. B **33**, 7346 (1986).

[7] H. Xu, J. Appl. Phys. **72**, 3522 (1992); Phys. Rev. B **46**, 12 251 (1992).

[8] M. Skowronski, Phys. Rev. B **46**, 9476 (1992).

[9] S. Dannefaer and D. Kerr, J. Appl. Phys. **60**, 591 (1986); S. Dannefaer, P. Mascher, and D. Kerr, J. Phys. Condens. Matter **1**, 3213 (1989).

[10] D. Pons and J. C. Bourgoin, J. Phys. C. **18**, 3839 (1985).

[11] R. Car and M. Parrinello, Phys. Rev. Lett. **55**, 2471 (1985).

[12] R. O. Jones and O. Gunnarsson, Rev. Mod. Phys. **61**, 689 (1989).

[13] G. B. Bachelet, D. R. Hamann, and M. Schlüter, Phys. Rev. B **26**, 4199 (1982); R. Stumpf, X. Gonze, and M. Scheffler (unpublished).

[14] L. Kleinman and D. M. Bylander, Phys. Rev. Lett. **48**, 1425 (1982).

[15] D. M. Ceperley and B. J. Alder, Phys. Rev. Lett. **45**, 566 (1980); J. Perdew and A. Zunger, Phys. Rev. B **23**, 5048 (1981).

[16] L. Gilgien, G. Galli, F. Gygi, and R. Car, Phys. Rev. Lett. **72**, 3214 (1994).

[17] A. Garcia and J. E. Northrup, Phys. Rev. Lett. **74**, 1131 (1995).

[18] U. Scherz and M. Scheffler, in *Imperfections in III/V Materials*, edited by R. Weber (Academic Press, New York 1993), pp. 2–58.

[19] J. S. Blakemore, J. Appl. Phys. **53**, R123 (1982).

[20] M. Saito and A. Oshiyama, Phys. Rev. Lett. **73**, 866 (1994).

[21] M. J. Puska, A. P. Seitsonen, and R. M. Nieminen, Phys. Rev. B **52**, 10 947 (1995).

[22] *Handbook of Chemistry and Physics*, 67th ed., edited by R. C. Weast (Chemical Rubber, Boca Raton, FL, 1986), p. D-68.

[23] J. E. Northrup and S. B. Zhang, Phys. Rev. B **47**, 6791 (1993); B.-H. Cheong and K. J. Chang, *ibid.* **49**, 17 436 (1994).

[24] T. Y. Tan, U. Gösele, and S. Yu, Crit. Rev. Solid State Mater. Sci. **17**, 47 (1991).